AGU PUBLICATIONS

JGR

Journal of Geophysical Research: Atmospheres

RESEARCH ARTICLE
10.1002/2014JD022645

Key Points:
- Extreme rainfall patterns from coupled air-sea modeling and observations
- River flooding and local ocean freshening in the Philippines
- MJO and synoptic events interact with terrain

Correspondence to:
J. Pullen,
Julie.Pullen@Stevens.edu

Citation:
Pullen, J., A. L. Gordon, M. Flatau, J. D. Doyle, C. Villanoy, and O. Cabrera (2015), Multiscale influences on extreme winter rainfall in the Philippines, *J. Geophys. Res. Atmos.*, *120*, doi:10.1002/2014JD022645.

Received 29 SEP 2014
Accepted 22 MAR 2015
Accepted article online 26 MAR 2015

Multiscale influences on extreme winter rainfall in the Philippines

Julie Pullen[1], Arnold L. Gordon[2], Maria Flatau[3], James D. Doyle[3], Cesar Villanoy[4], and Olivia Cabrera[4]

[1]Stevens Institute of Technology, Hoboken, New Jersey, USA, [2]Lamont-Doherty Earth Observatory, Columbia University, Palisades, New York, USA, [3]Naval Research Laboratory, Monterey, California, USA, [4]Marine Science Institute, University of the Philippines-Diliman, Quezon City, Philippines

Abstract During 2007–2008, the Philippines experienced the greatest rainfall in 40 winters. We use a combination of observations (including 48 meteorological stations distributed throughout the islands, Tropical Rainfall Measuring Mission satellite-sensed precipitation, and shipboard measurements) along with a high-resolution two-way coupled ocean/atmosphere model (3 km Coupled Ocean-Atmosphere Mesoscale Prediction System (COAMPS)®) to examine this anomalous season. As expected from climatology, rainfall was greatest on the eastern side of the archipelago, with seasonal totals exceeding 4000 mm in some locations. A moderate to strong La Niña increased the rainfall across the region. But discrete precipitation events delivered the bulk of the rain to the area and coincided with intense Madden-Julian oscillation activity over the archipelago and a late February cold surge. General patterns and magnitudes of rainfall produced by the two-way coupled model agreed with observations from land and from space. During the discrete events, the 3 km COAMPS also produced high amounts of precipitation in the mountainous parts of central Philippines. Direct observations were limited in this region. However, the government reported river flooding and evacuations in Mindoro during February 2008 as a result of significant rainfall. In addition, shipboard measurements from late January 2008 (collected by the Philippines Straits Dynamics Experiment) reveal a fresh lens of water to the west of the island of Mindoro, consistent with high freshwater discharge (river runoff) into the coastal area.

1. Introduction

1.1. MJO and the Maritime Continent

The Madden-Julian oscillation (MJO) is a source of intraseasonal variability for the globe [*Madden and Julian*, 1971; *Zhang*, 2005]. With its origin in the Indian Ocean and subsequent eastward propagation, the MJO has a particular impact on the tropical regions of the Indian and Pacific Oceans. The MJO signal has a 30–60 day period, is strongest during the northern hemisphere winter [*Chen and Yanai*, 2000], and carries enhanced deep convection. The associated alternating wet and dry phases each lasts approximately several days to a week.

Processes operating on multiple time and space scales are involved in the coupled ocean-atmosphere phenomena constituting the MJO [*Ichikawa and Yasunari*, 2007; *Majda and Stechmann*, 2009]. The Indian Ocean Dipole (IOD) characterizes the strength of the west (warm) to east (cold) gradient in sea surface temperature (SST) anomalies across the basin and has been shown to impact the MJO. The Dipole Mode Index (DMI) being neutral to negative (warmer waters in the eastern Indian Ocean) is linked with enhanced MJO activity over the Maritime Continent (which encompasses Indonesia, The Philippines, and Papua New Guinea [*Ramage*, 1968]), via the warmer surface waters in the eastern Indian Ocean increasing moisture in the atmospheric flow [*Wilson et al.*, 2013].

As the MJO propagates across the Maritime Continent, there is significant interaction with synoptic events and topographic features [*Wu and Hsu*, 2009]. The seasonal wintertime prevailing northeast monsoon is frequently intensified by synoptic cold surges that sweep down from the South China Sea several times per month. Strong to moderate cold surges are suspected to act as a catalyst or intensifier for MJO initiation and subsequent propagation across the Maritime Continent [*Chang et al.*, 2004; *Wang et al.*, 2012] and can occur at any phase of the MJO. However, there is some suggestion that weak cold surges are inhibited during the early stages (1 and 2) of the MJO due to countervailing winds [*Chang et al.*, 2005a]. An analysis of 10 winters (December 2000–March 2009) showed that the combined northerly surge/MJO pattern (16 cases) produced much greater precipitation over the Maritime Continent than

either MJO (20 cases) or northerly surge (11 cases) alone [*Hattori et al.*, 2011]. Areas of appreciably enhanced precipitation were found in the western and northwestern parts of Java as well as the eastern Philippines.

A detailed analysis of the unfolding of several events provides an appreciation of how variability on multiple time scales can lead to anomalous outcomes. Using Tropical Rainfall Measuring Mission (TRMM) SST and precipitation retrievals, *Tangang et al.* [2008] describe how the once in a century flood of the southern Malaysian peninsula in winter 2006/2007 was the result of several distinct precipitation events triggered by the confluence and subsequent modulation of the MJO, cold surge, and Borneo vortex—and interaction with terrain. In the first episode, easterly winds over Java were a result of the (phase 1) MJO and served to advance the northeasterly surge to the Malaysian peninsula, farther south than normal. Once there, low-level convergence triggered by the flow impinging on steep terrain created enhanced precipitation.

Most recently, increased rainfall at the regional and local levels has been associated with MJO propagation through the Maritime Continent. *Xavier et al.* [2014] employed TRMM and rain gauge data over Southeast Asia for 1998–2012 to show that the occurrence of extreme rain events increased by 30–50% during convective MJO phases, and the signal was evident locally in Singapore. *Wu et al.* [2013] used precipitation land-based radar to confirm a 4 day extreme rain event on western Java Island and link it to a wet phase of the prevailing MJO. In Papua New Guinea, approximately 30% more rain was observed to fall in the mountains during the wet phase of the MJO [*Matthews et al.*, 2013]. And this signal was evident in gauged water levels in the rivers that drained the mountains.

1.2. Modeling and Prediction of MJOs

Accurate MJO forecasting is a relatively recent endeavor. Since the MJO is a large-scale planetary oscillation, the task of MJO simulation has typically fallen to general circulation models (GCMs). More recently, a series of studies has produced increased realism in MJO initiation, propagation speed, variance, and predictability using enhancements to GCMs. On climate time scales, there was a marked improvement of MJO representation in models included in the Coupled Model Intercomparison Project phase 5 (CMIP5) compared to CMIP3 [*Hung et al.*, 2013], with CMIP5 models exhibiting larger MJO variance and more realistic ratio of eastward/westward propagation. The simulation of the convectively coupled equatorial waves was also improved. Nevertheless, the simulation of MJO still poses a significant challenge, due to the sensitivity to model physics—especially the representation of moisture and deep and shallow convection. It appears that employing the "superparameterization" [*Grabowski*, 2006] that resolves the two-dimensional structures of the subgrid clouds [e.g., *Benedict and Randall*, 2009] or explicit representation of cloud processes on a high-resolution grid [*Miura et al.*, 2007] improves the MJO simulation.

In the extended weather forecasting context, specific model improvements have been attained for the genesis and early propagation phases of the MJO utilizing multiple global and regional models, along with coordinated forecasting and skill assessment for operational products [*Gottschalck et al.*, 2010]. MJO forecasting strongly depends on MJO phase, with initiation in the Indian Ocean and propagation through the Maritime Continent having the weakest skills. The 2010–2012 Cooperative Indian Ocean Experiment on Intraseasonal Variability in Year 2011 (CINDY2011)/Dynamics of the MJO (DYNAMO) field and modeling campaign focused on improving MJO observation and prediction [*Yoneyama et al.*, 2013] during the initiation in the Indian Ocean. *Fu et al.* [2013] examined the MJO forecast during the DYNAMO (Dynamics of the MJO)/CINDY (Cooperative Indian Ocean Experiment on Intraseasonal Variability in Year 2011) and found that the MJO predictability ranged from 13 days in the Global Forecast System atmosphere-only model to 36 days in a multimodel ensemble.

Atmospheric GCM (AGCM) simulations display a strong sensitivity of simulated MJO characteristics to the specified SST. There is a spate of research demonstrating that the MJO is a two-way coupled phenomenon [*Flatau et al.*, 1997; *Aldrian et al.*, 2005; *Zhang et al.*, 2006; *Kim et al.*, 2008; *Fu et al.*, 2008; *Woolnough et al.*, 2007]. Generally, these studies couple an AGCM to ocean models possessing varying degrees of complexity and show that the coupled results improve the modeled MJO phase speed and intensity. One such study used a coupled GCM (National Centers for Environmental Prediction (NCEP) Climate Forecast

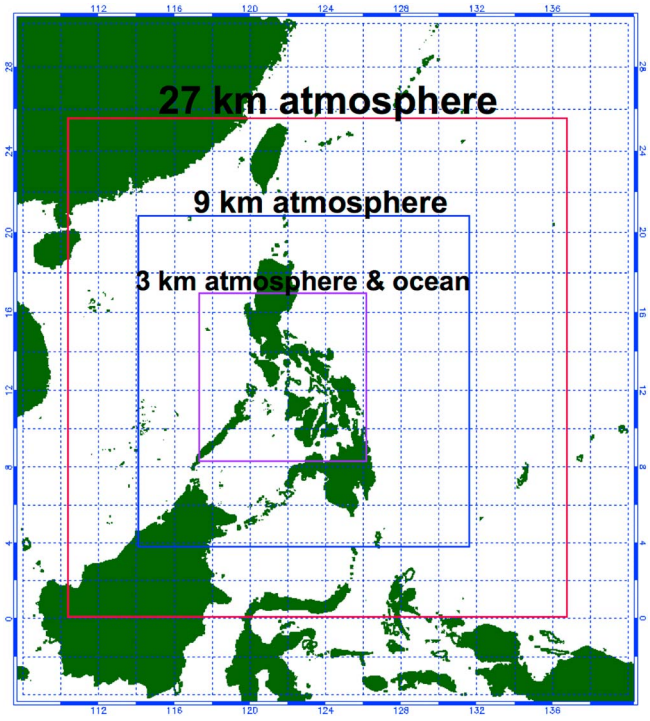

Figure 1. COAMPS nested grid configuration.

System with T62 atmospheric resolution and 1/3°×1° oceanic resolution) to extend predictability of the MJO by 10 days [*Pegion and Kirtman*, 2008a, 2008b].

In spite of significant progress in MJO prediction, the "predictability barrier" of MJO propagation through the Maritime Continent still constitutes the formidable forecasting challenge. Most recently, *Xavier et al.* [2014] utilized the Met Office Global Seasonal forecasting system to demonstrate skillful probabilistic prediction of MJO-derived extreme rain events at medium range for the Southeast Asian region. Nevertheless, due to resolution limitations, such systems typically underresolve terrain and significantly underpredict rainfall on land. Topographic blocking and channeling during synoptic events (e.g., cold surges) and MJO passages, associated enhanced rainfall, and SST variability on small scales are ubiquitous features of the Maritime Continent. Additionally, the combined and sometimes unexpected effects of synoptic and intraseasonal interactions (and their sensitivity to terrain) are emerging as important topics based on relatively coarse grain observational and reanalysis evidence [*Hattori et al.*, 2011]. Recent atmospheric modeling studies at varying resolutions for Malaysia (15 km) [*Juneng et al.*, 2007], Taiwan (2 km) [*Chen et al.*, 2013], and Madeira (1 km) [*Couto et al.*, 2012] have examined orographic effects on extreme precipitation during synoptic events. But these topics have not been explored within the context of a high-resolution two-way coupled model. In particular, no modeling study to date has investigated the linkage of small-scale precipitation in mountainous tropical regions of the Maritime Continent with MJO and other factors.

As part of the Office of Naval Research (ONR)-sponsored Philippine Straits Dynamics Experiment (PhilEx) [*Gordon et al.*, 2011], several research cruises occupied the Philippine Archipelago during 2007 to 2009. Despite being the dry season, boreal winter 2007–2008 produced excessive precipitation in the Philippines [*Gordon et al.*, 2011]. In this work we examine the conditions that created the extreme precipitation, utilizing high-resolution (3 km) two-way coupled ocean-atmosphere modeling, along with observational data sets derived from ocean measurements, remote sensing, and land-based rain gauges. Our work seeks to illuminate the modulation of rainfall caused by different multiscale and orographic factors and their interaction. In this study we examine the surface characteristics of patterns influenced by the various

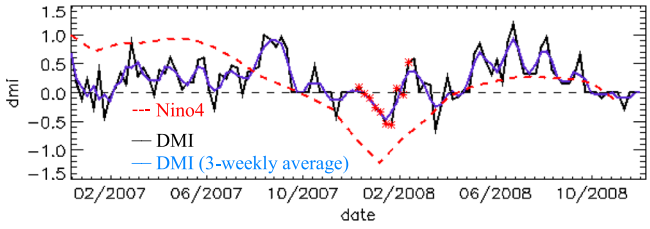

Figure 2. Weekly Dipole Mode Index (DMI) (black line) and 3 weekly averaged (blue line). The period with anomalous rainfall, and when the DMI is negative to neutral, is indicated with red stars. The red dashed line is the Niño4 index, based on monthly data (with 28 subtracted off to scale to the DMI range). Negative Niño4 values represent La Niña conditions.

factors. Section 2 describes the model and data sets, section 3 discusses the multiscale factors that were operative during the time period of interest, while section 4 describes the rainfall and salinity patterns. The conclusions are contained in section 5.

2. Methods

2.1. TRMM

The Tropical Rainfall Measuring Mission (TRMM) precipitation radar data are employed in this analysis. TRMM multisatellite precipitation analysis 3B42RT combines microwave (less frequent but more accurate) and infrared (more frequent but less accurate) satellite-based sources [*Huffman et al.*, 2007]. The data set blends microwave data from the TRMM Microwave Imager, Advanced Microwave Scanning Radiometer for Earth Observing System, Advanced Microwave Sounding Unit-B, Special Sensor Microwave Imager, with infrared data from geosynchronous Earth orbit satellites. The spatial resolution is

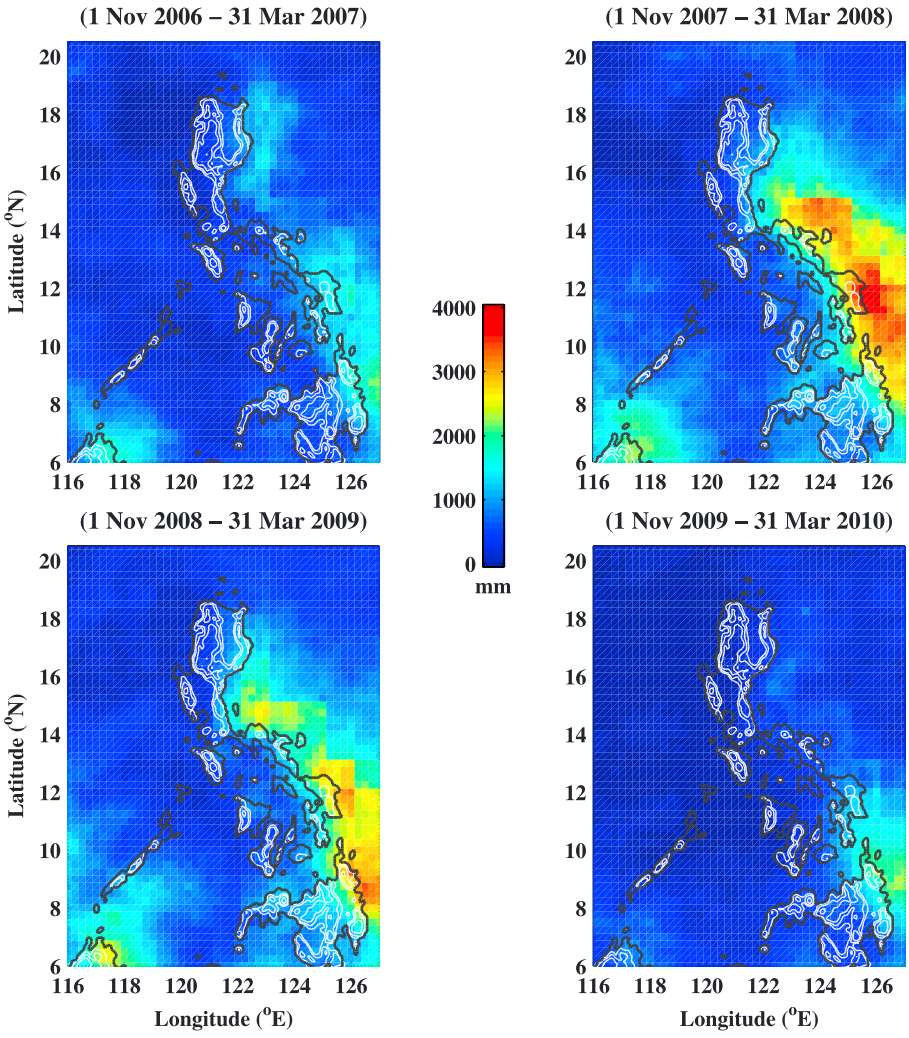

Figure 3. TRMM satellite rainfall totals for 1 November to 31 March of four consecutive years. Terrain is contoured in white at elevation levels 250, 500, 1000, and 2000 m.

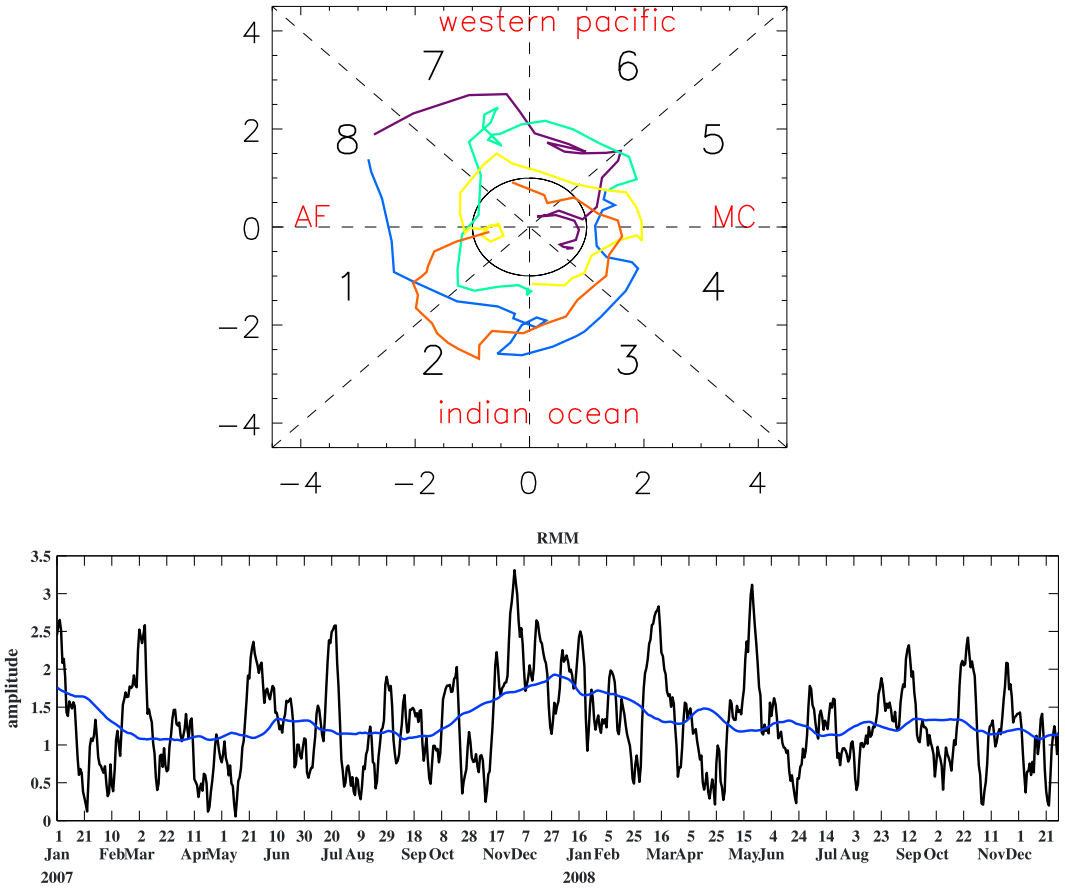

Figure 4. (top) Wheeler-Hendon diagram for 11 November 2007 to 31 March 2008 showing the amplitude and phasing of MJO for November 2007 (purple), December 2007 (blue), January 2008 (green), February 2008 (yellow), and March 2008 (orange). MC is Maritime Continent. AF is western hemisphere and Africa. (bottom) RMM amplitude in black, with the 90 day running mean in blue.

0.25° with 3 hourly temporal resolution. TRMM data are utilized for 1 November 2006 to 31 March 2010, with a particular focus on 1 November 2007 to 31 March 2008 (Figure 3).

2.2. Rain Gauge

Rain gauge data from 48 station sites throughout the Philippines were compiled by the Philippine Atmospheric, Geophysical and Astronomical Services Administration (PAGASA). The data set was processed at a 3 hourly rate and covers the 5 month time period 1 November 2007 to 31 March 2008. Station locations are shown in Figure 7.

2.3. Ship-Based Measurements

Ship-based conductivity-temperature-depth (CTD) measurements were made as part of the PhilEx program on two regional Intensive Observational Period (IOP) research cruises in January 2008 (IOP-08) and March 2009 (IOP-09) [*Gordon and Villanoy*, 2011; *Gordon et al.*, 2011]. CTD casts were also performed during the Joint U.S./Philippines research cruise of November and December 2007. All measurements were made from the R/V *Melville*, and many of the same stations were occupied in each cruise.

2.4. Model

The Coupled Ocean-Atmosphere Mesoscale Prediction System (COAMPS) is used for this study. The atmospheric model is nonhydrostatic and possesses a terrain-following vertical coordinate [*Hodur*, 1997]. The ocean model, the Navy's Coastal Ocean Model (NCOM), features hydrostatic dynamics, and a bathymetry following vertical coordinate [*Barron et al.*, 2006]. The Earth System Modeling Framework provides the model coupling framework [*Allard et al.*, 2010]. The ocean and atmosphere model exchange flux information every 12 min.

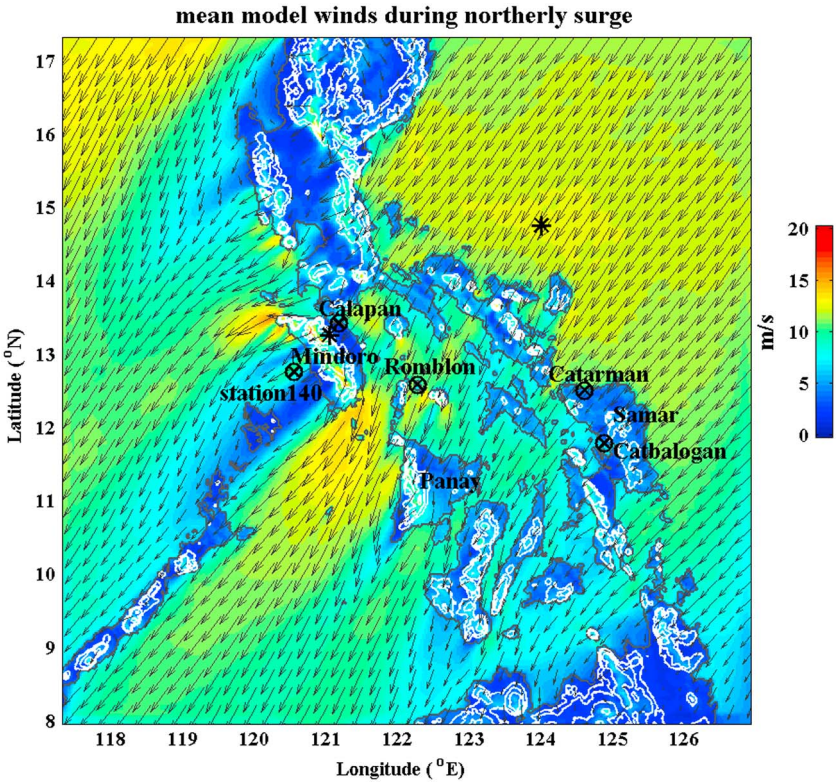

Figure 5. COAMPS 3 km resolution mean wind speed for the northerly surge of 9–16 February 2008. Wind vectors and magnitude (color shaded) are shown. Labeled are the islands of Mindoro, Panay, and Samar and the stations Romblon, Calapan, Catbalogan, Catarman, and the offshore sampling station 140. The asterisks show sites extracted from the model on the island of Mindoro (with the highest model rainfall) and on the upwind side of the Philippines. Statistics are given in the text for these sites. Terrain is shown as in Figure 3.

The COAMPS model has previously been run and evaluated for the Philippines region in both forecast and hindcast modes [*Pullen et al.*, 2011]. COAMPS simulation results for MJOs demonstrate skill in propagating the MJO signal through the domain [*Shinoda et al.*, 2013]. Coupled COAMPS with nested grids and the highest-resolution grid centered on the DYNAMO observational array was used to model the MJOs observed from October to December 2011. *Chen et al.* [2015] examined the moisture resurgence preceding the MJO formation and found that the coupled COAMPS forecasts show good agreement with observations gathered during the DYNAMO IOP.

In the current simulations, the atmosphere model resolution is nested to 27/9/3 km and the ocean model resolution is nested 3/1 km. The 1 km ocean grid results are presented in *May et al.* [2011]. Here we utilize the 3 km resolution model grid output with two-way coupling (Figure 1). The ocean and atmosphere each have 40 vertical levels. Model initiation comes from Navy Operational Global Atmospheric Prediction System (atmosphere) and global NCOM (ocean). Subsequently, the ocean model is free running, and the atmosphere model uses multivariate optimal interpolation data assimilation with a twice daily update cycle. The model fields are available for 15 January to 1 March 2008. Additional details of the specific model implementation used in this study can be found in *May et al*. [2011].

3. Multiscale Factors

3.1. El Niño–Southern Oscillation (Interannual)

The region experienced a moderately strong La Niña that peaked in January and February 2008 (Figure 2, red dashed lines). The peak timing of this La Niña was later than typical [*Wheeler*, 2008]. This La Niña was the biggest since 1988 and the fourth strongest since 1950 using the Troup Southern Oscillation Index, Niño3.4 Index, and Multivariate El Niño–Southern Oscillation Index [*Wheeler*, 2008]. When La Niña conditions occur, the impact on the Philippines is elevated rainfall throughout the archipelago [*Lyon et al.*, 2006]. That study utilized a seasonal long-term average at 40 stations from 1951 to 2004 and showed the

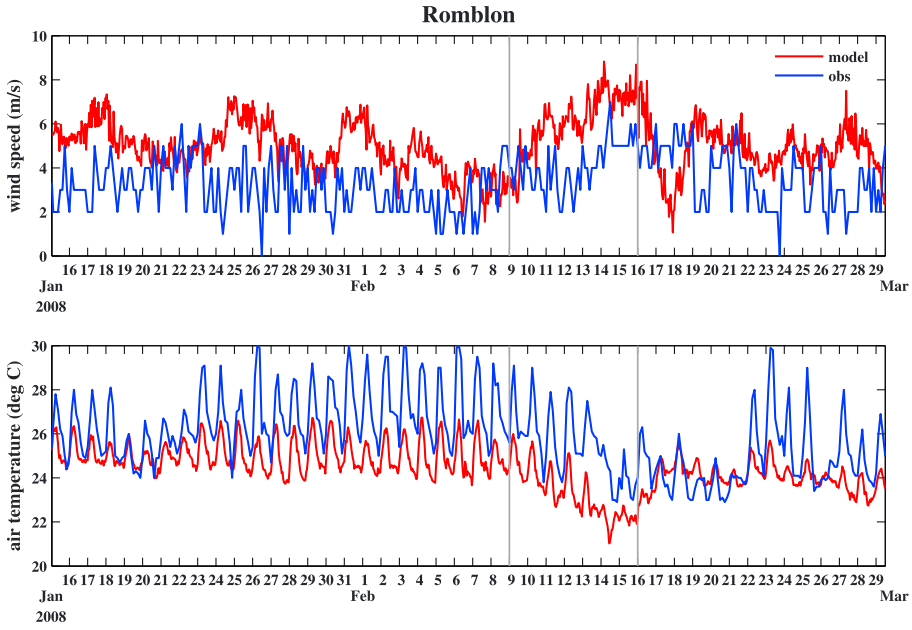

Figure 6. Modeled and observed wind speed and air temperature at station Romblon. (See Figure 5 for location.) The gray lines delineate the time period of the northerly surge (9–16 February 2008).

pattern to be statistically significant at the 95% level for all stations and contrasts with reduced rainfall at all stations in the summer during La Niña [*Lyon and Camargo*, 2009].

3.2. IOD (Ocean/Interannual)

Ocean temperatures are known to drive global variability in the atmosphere on multiple time scales. The Indian Ocean Dipole is defined as anomalies in SST that create a pattern of warmer waters in the western

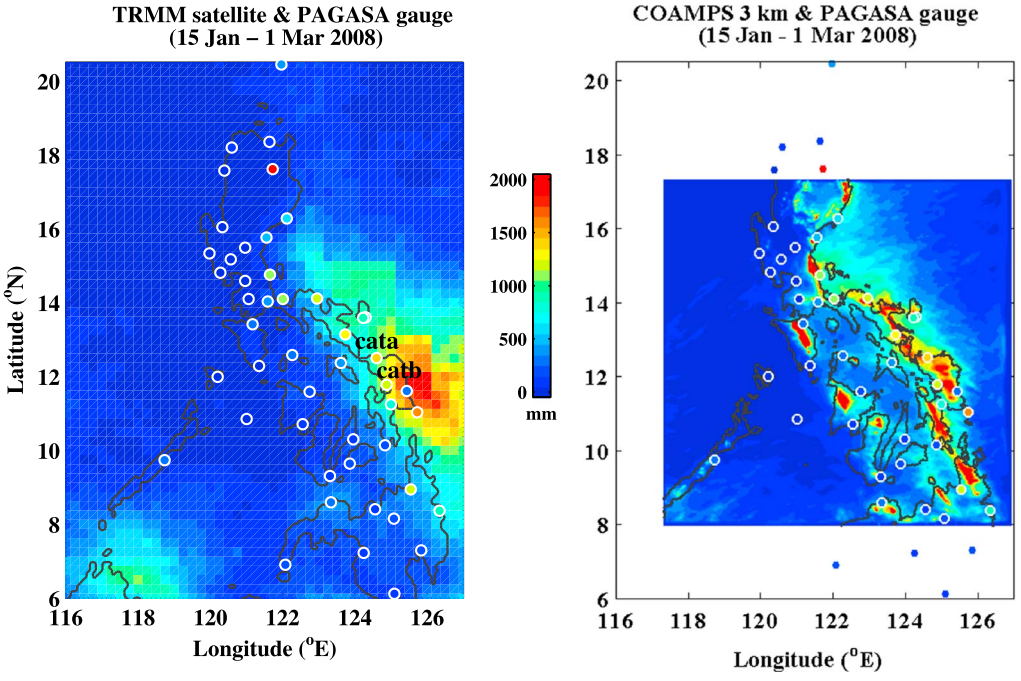

Figure 7. (left) TRMM satellite and PAGASA gauge rainfall totals (circles) for 15 January to 1 March 2008. (right) COAMPS and PAGASA gauge rainfall totals (circles) for the same time period.

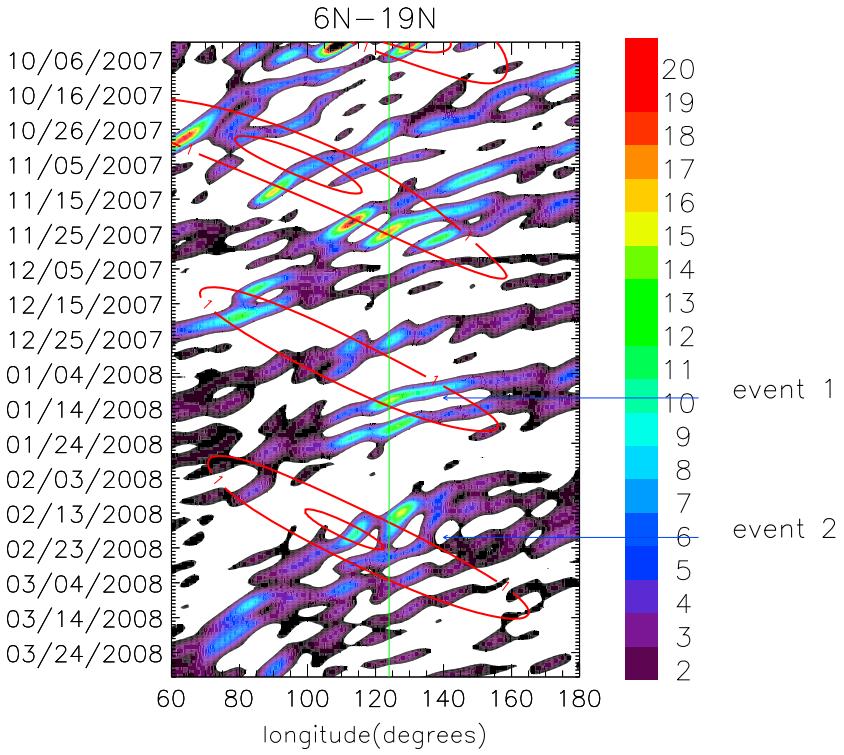

Figure 8. Time-longitude plot of the TRMM precipitation in mm/d averaged between 6 and 19°N. The shading indicates westward propagating component of precipitation with periods between 3 and 40 days and zonal wave numbers 1–40. The red contours indicate the low-frequency (intraseasonal) component, with a period of 40–80 days and zonal wave numbers 1 to 6. The longitude of the Philippines is ~118 to 126, approximated by the blue vertical line at 125. MJO events 1 and 2 are shown with blue arrows and labeled.

Indian Ocean and cooler waters in the eastern Indian Ocean. The Dipole Mode Index (DMI) being neutral to negative (warmer waters in the eastern Indian Ocean) is more common during La Niña [*Allan et al.*, 2001]. During the period of anomalous rainfall in November to February 2007–2008, the DMI was negative to neutral (Figure 2). Negative to neutral IOD is also associated with enhanced MJO activity over the Maritime Continent [*Wilson et al.*, 2013].

3.3. Northeasterly Monsoon (Seasonal)

The climatological monthly mean rainfall values in the Philippines based on Association of Southeast Asian Nations Climatic Atlas Project data from 1902 has a pronounced east-west gradient in winter [*Chang et al.*, 2004, 2005b]. The northeasterly monsoon (November to April) moistens, transiting the ocean due to the sea surface fluxes. In encountering the Philippine topography downwind, orographic lifting consisting of upslope flow and precipitation on the windward (eastern) side of the islands ensues. The downstream side of the islands experiences a rain shadow. This pattern is borne out by a refined analysis employing data from 41 PAGASA stations from 1961 to 2000 [*Akasaka et al.*, 2007] and 35 stations from 1951 to 2010 [*Villafuerte et al.*, 2014]. In those analyses, the east coast of the Philippines was influenced more by the northeasterly (winter) monsoon than the southwesterly (summer) monsoon. Rainfall totals there begin to increase from early October to December and show the characteristic east-west gradient across the archipelago.

The Philippines experienced exceptionally high rainfall during 1 November 2007 to 31 March 2008 (Figure 3). Compared to adjacent years, average rainfall was 30–75% higher. All years shown depict rain concentrated on the east coast, consistent with previous studies [*Chang et al.*, 2004; *Akasaka et al.*, 2007].

3.4. MJO (Intraseasonal)

Intraseasonal variability in winter 2007–2008 was particularly intense. The classic Wheeler-Hendon plot [*Wheeler and Hendon*, 2004] shows the prevalence of MJO during November 2007 through March 2008 (Figure 4, top).

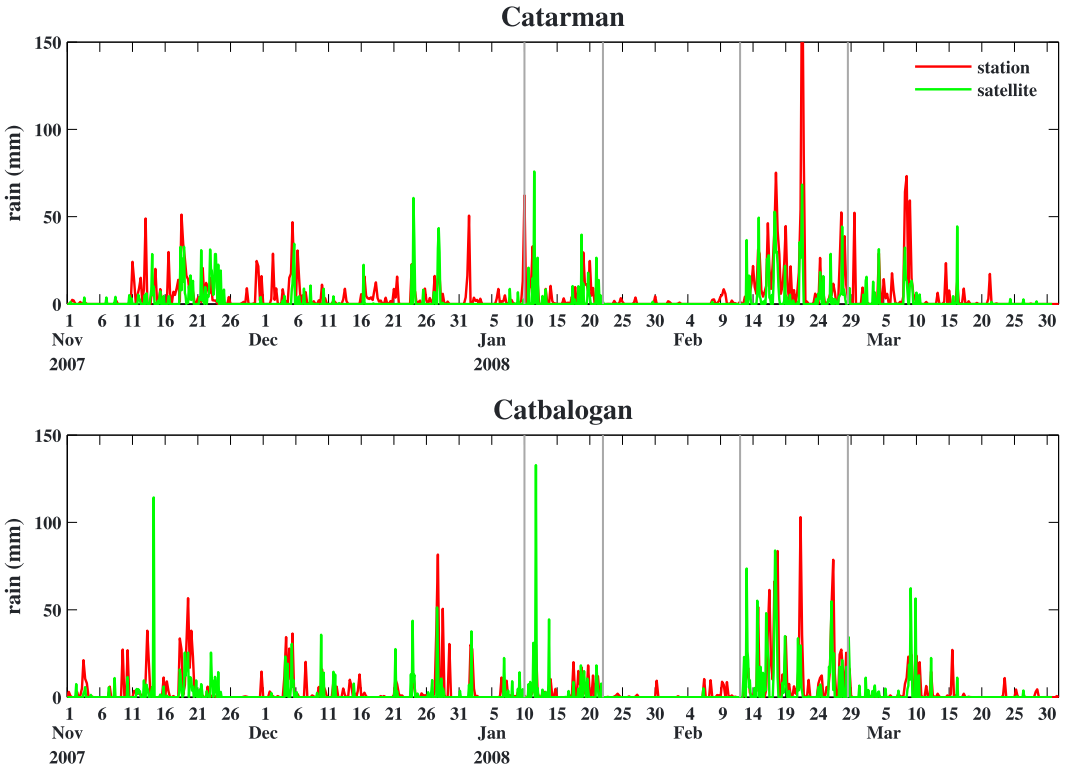

Figure 9. Time series for satellite (green) and station (red) rainfall for 1 November 2007 to 31 March 2008. The station locations for Catarman and Catbalogan are shown in Figures 5 and 7. The two MJO periods highlighted in the text are shown with gray lines. These are 10–22 January (event 1) and 12–28 February (event 2).

MJO phases 4 through 6/7 can produce rainfall over the Philippines, and these combined phases last typically 12–15 days [*Peatman et al.*, 2013]. In the real-time mutivariate MJO (RMM) principal components of winds aloft and outgoing longwave radiation (OLR) data, RMM1 and RMM2 represent the time variation of the components. RMM amplitude (Figure 4, bottom) greater than 1 connotes significant MJO activity. This level was attained mid-November 2007 through the end of March 2008. The maximum amplitude, exceeding 3, was achieved in early December when the MJO event was in its early stages in the western Indian Ocean. January and February 2008 produced MJO activity in the Philippine area with RMM amplitude exceeding 1. In the context of prior years, RMM amplitude in winter 2008 was the greatest since 2005 [*Wheeler*, 2008].

Two intraseasonal oscillation events of winter 2007–2008 documented by *Lin* [2012] originated off the tip of Africa and bifurcated at the Maritime Continent—consisting of a northeast propagating band of activity (over the Philippines) and a southeast extending band. The initiation of the second event in late January (what became event 2 below) has been linked to a prior cold surge as an important precursor [*Wang et al.*, 2012].

3.5. Cold Surge (Synoptic)

During February 2008, an intense cold surge impacted the Philippines. Intensifications in the northeasterly monsoon can occur several times a month and are generated by displacements in the Siberian-Mongolian High over Asia [*Chang et al.*, 2006]. Details of the impact of cold surges on the ocean and atmosphere circulation around the Philippines can be found in *Pullen et al.* [2008]. The cold surge lasted from 9 to 16 February 2008 in the Philippines, had a northerly orientation, and was stronger and longer than typical cold surges [*Pullen et al.*, 2011]. The surge occurrence was verified in QuikSCAT fields for the Philippines [*Pullen et al.*, 2011] and has also been documented in studies of the South China Sea region [*Hong and Li*, 2009].

In the COAMPS simulation, oncoming winds reached a maximum speed of 16 m/s upstream of the Philippines (marked by an asterisk in Figure 5), with a mean wind over the 8 day event of 12 m/s. The standard deviation in that same location was 2.4 m/s, suggesting relatively steady and strong winds during the event. Strong winds and cold air temperatures were measured at station Romblon (see Figure 5 for location) during the cold surge

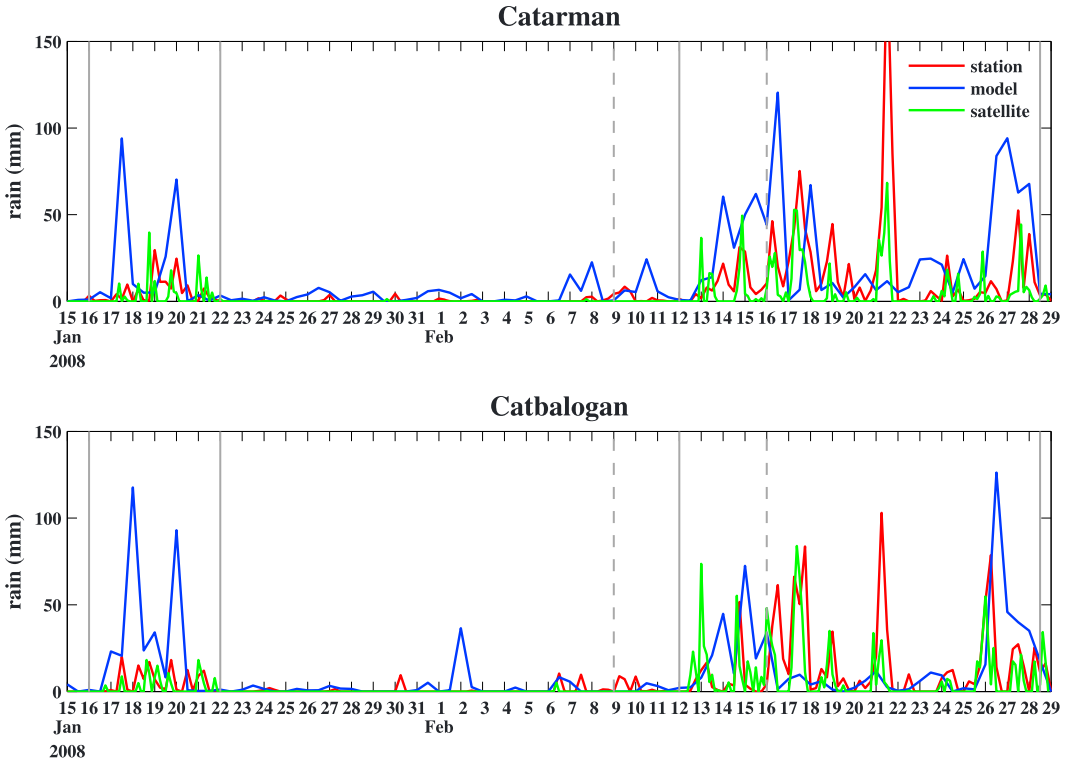

Figure 10. Station rainfall values from three sources: satellite, model, and rain gauge at (top) the Catarman and (bottom) Catbalogan. See Figures 5 and 7 for station locations. The solid gray lines denote MJO event 1b and event 2. The time period of the northerly cold surge is shown with dashed gray lines.

(Figure 6). (Measured winds were reported to the nearest unit digit.) The shift was also evident in the COAMPS model fields at the same site. During the northerly surge, the maximum wind speed at Romblon was 7 m/s (observed) and 8.8 m/s (modeled), while the minimum air temperature dropped to 22.9°C (observed) and 21°C (modeled).

Although surges start out cooler and drier, they pick up moisture flowing across the warmer waters of the South China Sea [*Chang et al.*, 2005a]. During January and February 2008, ocean surface temperatures to the east of the Philippines were approximately 28°C. Temperatures were anomalously warmer by ~1.0–1.5°C during this moderate to strong La Niña year [*Wheeler*, 2008]. Low-level convergence is evident near the coast, particularly in the vicinity of Samar (Figure 5), leading to enhanced convection during a surge [*Tangang et al.*, 2008]. Further deep convection occurs downstream in the Maritime Continent due to blocking by terrain [*Chang et al.*, 2005a].

4. Rainfall and Salinity Patterns

TRMM satellite-derived precipitation totals are compared with in situ rain gauge data and COAMPS fields for the time period of 15 January to 1 March 2008 (Figure 7). For this reduced time period beginning mid-January, the TRMM fields still reveal the expected pattern of highest rainfall on the eastern side (although values are

Table 1. Rainfall Totals (in Millimeter) at Three Stations for Event 1b and Event 2

	Catarman		Catbalogan		Calapan	
	Event 1b	Event 2	Event 1b	Event 2	Event 1b	Event 2
Satellite	160	881	133	1173	17	25
Gauge	137	1151	125	996	94	160
Model	226	978	324	577	65	399

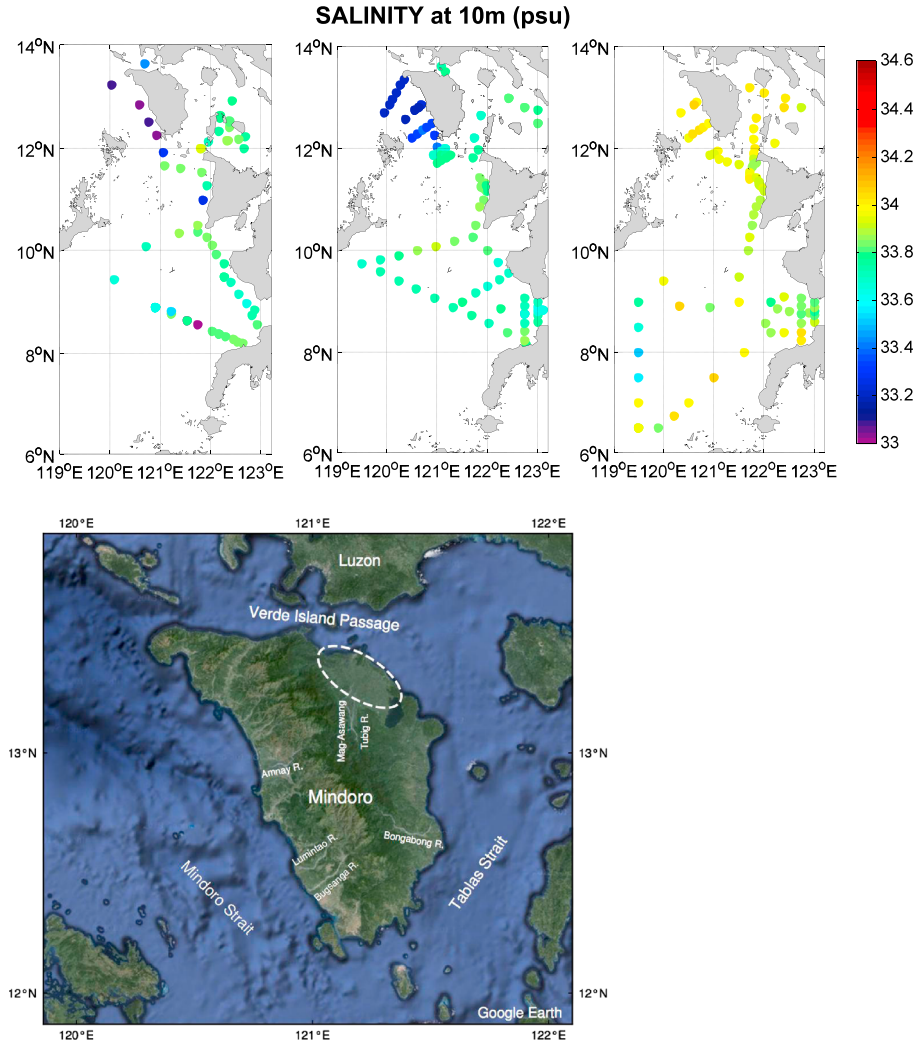

Figure 11. (top) Shipboard in situ salinity measurements at 10 m depth from (left) December 2007, (middle) January 2008, and (right) March 2009 (after *Cabrera* [2012]). (bottom) Rivers draining the highlands of Mindoro Island. The circle denotes the approximate region of evacuations that occurred on 19 February 2008.

approximately half those of the longer time period represented in Figure 3). The rain measured by the rain gauges is similar in magnitude and distribution to the satellite fields, but in coastal and central portions of the Philippines, the gauges report rain in areas not measured by TRMM. Indeed, rainfall retrieved from TRMM has challenges over complex terrain and issues with uncertain attenuation correction [*Barros et al.*, 2000; *Iguchi et al.*, 2000]. Other studies have documented that TRMM underestimates rainfall in the interior and overestimates rainfall at the coast compared with in situ measurements [*Kanamori et al.*, 2013]. For the Philippines, *Jamandre and Narisma* [2013] revealed poor correlation of TRMM with eight rain gauge stations over 2003–2005, with greatest discrepancies occurring in the west and south of the country. Moreover, TRMM underestimated Philippine rain events (>20 mm) by ~50%.

COAMPS rain totals (extracted at the nearest model grid point to the station location) on the east coast roughly reproduce the patterns observed, but the rain is tied more closely to the coastline than the TRMM data. Rainfall totals in the coastal regions tend to match the rain gauge data. Of particular note are the elevated values that the model produces in the mountainous regions of Mindoro and Panay islands. These will be examined in more detail.

The timing of the rain episodes associated with MJO is found from the low-frequency (intraseasonal) component of TRMM rain rate (Figure 8). Discrete precipitation events on 15–25 November 2007, 10–22 January (event 1),

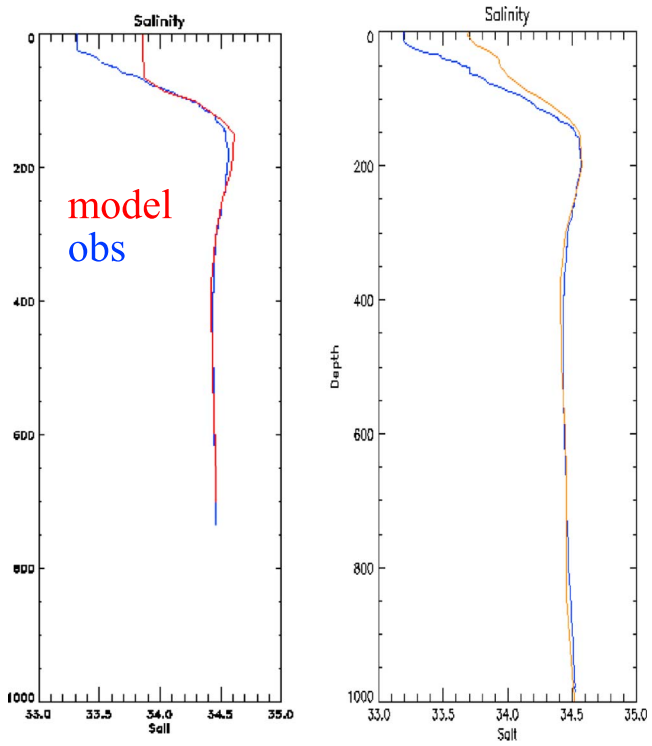

Figure 12. Salinity from CTD casts at two stations (blue) during the January 2008 PhilEx cruise on the R/V *Melville*. The location of the cast is shown in Figure 11. Modeled salinity at the same time and location is shown (red).

and 12–28 February 2008 (event 2) are evident. Westward moving systems often emanate from MJO, particularly on the trailing end of an event [*Nakazawa*, 1988]. This is apparent in the January period. For subsequent analysis, the January event can be separated into two distinct periods of rain from 10–14 January (event 1a) and 16–22 January (event 1b).

Time series of TRMM and PAGASA rain gauge data at two sites on the east side of the Philippines (Catarman and Catbalogan locations shown in Figures 5 and 7) showed clear episodic rain events in the periods indicated by the TRMM phasing (Figure 9). The last two events, event 1 in January and event 2 in February, are marked with gray lines. There is a general agreement in the amount and timing of the rainfall between the two observation modalities, especially at Catarman during event 1 and at Catbalogan during event 2. At both stations, the three discrete rainbands of event 2 (shown in Figure 8) are clearly visible in both data sets.

The model fields for the period of 15 January to 1 March 2008 at the two station locations replicated the general trends of the satellite and gauge fields (Figure 10). Rainfall totals at the two stations were higher for event 2 relative to event 1 for the model and observations (Table 1). The model rainfall was higher than the gauge and satellite data for event 1b at both stations and lower for event 2 at Catbalogan. During event 2, the model showed an imprint of the first and third rainbands of the event but missed the second band.

Shipboard measurements of near-surface salinity on the west side of Mindoro revealed unusually low salinity (fresh) water, below 33.4, during the December 2007 and January 2008 cruises (Figure 11, top). Station 140, sampled on 26 January 2008, had a surface value of 33.1. For comparison, salinity values were higher and more homogeneous throughout the region (approximately 34) during the March 2009 cruise. The island of Mindoro consists of two high mountains, Mount Baco and Mount Halcon, each reaching ~1500 m. At least five rivers drain the mountains on the west side and discharge into the coastal waters (Figure 11, bottom). These rivers were not gauged. On 25 and 26 January 2008, CTD station locations 133 and 140 in the coastal waters off Mindoro measured a surface-intensified freshening whose influence extended to a depth of at least 75 m (Figure 12). The ocean model did not match the lower-salinity water near the surface but matched the profile at both stations at deeper depths. Although the ocean model can represent river runoff, for these simulations, coastal runoff was not incorporated since an accurate assessment of discharge was not available.

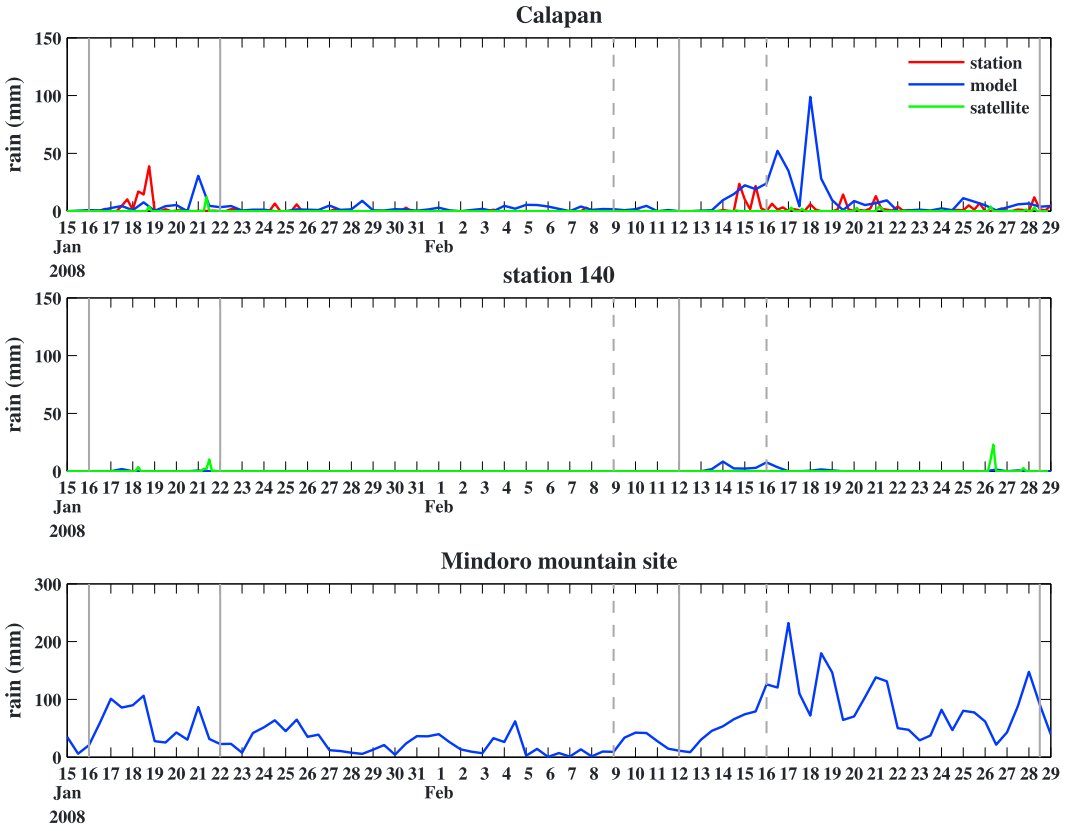

Figure 13. (top) Time series of rain at land station Calapan and (middle) offshore station 140 (located west of Mindoro). (bottom) Model precipitation at the site of greatest rainfall in the model located in the Mindoro mountains, shown with an asterisk in Figure 5. The gray solid lines show MJO event 1b and event 2, while the gray dashed lines delineate the time period of the northerly surge.

Strong spatial gradients in rainfall exist in and around Mindoro (Figure 13). As the west side of Mindoro is in the rain shadow of the island, surface freshening due to local precipitation is not expected. And indeed at station 140 offshore of Mindoro, the model and satellite showed no appreciable precipitation in the lee of Mindoro. Near the northeast coast of Mindoro at station Calapan, some rain was observed during events 1b and 2. At Calapan, the rainfall was overestimated by the model and was not discernible by satellite. A time series from the location on Mindoro with the most precipitation in the model (see Figure 5 for location) reveals that the bulk of the rain was delivered during event 1b (730 mm or 16%) and event 2 (2766 mm or 61%) (Figure 13), although rainfall may have been overestimated by the model. Thus, the MJO phasing is prominent in the timing of the extreme rainfall in Mindoro as well as on the eastern side of the archipelago. The two MJO events, event 1b lasting 7 days (16–22 January) and event 2 lasting 17 days (12–28 February), delivered over 75% of the rainfall of the 1.5 month model record under examination at the Mindoro mountain site.

Consistent with this model-derived extreme rainfall in the mountains, the Philippine government and news media reported that heavy rains caused river flooding and evacuations on the island of Mindoro (see Figure 11 (bottom) for approximate location of evacuations) on 19 February 2008 [*National Disaster Coordinating Council* (*NDCC*), 2008]. On 19 February 2008, news and government reports stated that in the town of Naujan, Oriental Mindoro Province, "nonstop rains in the mountain ranges of Oriental Mindoro caused the river Magasawang Tubig to overflow its banks, affecting 4300 families or a total of 15,828 persons (in 20 villages)" [Philippines Inquirer; *NDCC*, 2008].

Maps of modeled rainfall totals for event 1b reveal the relationship of model precipitation to terrain and coastline (Figure 14). The 3 km resolution model generated rain on the east coast as expected, with enhanced values to the southeast in accordance with climatological maps of rainfall in the region

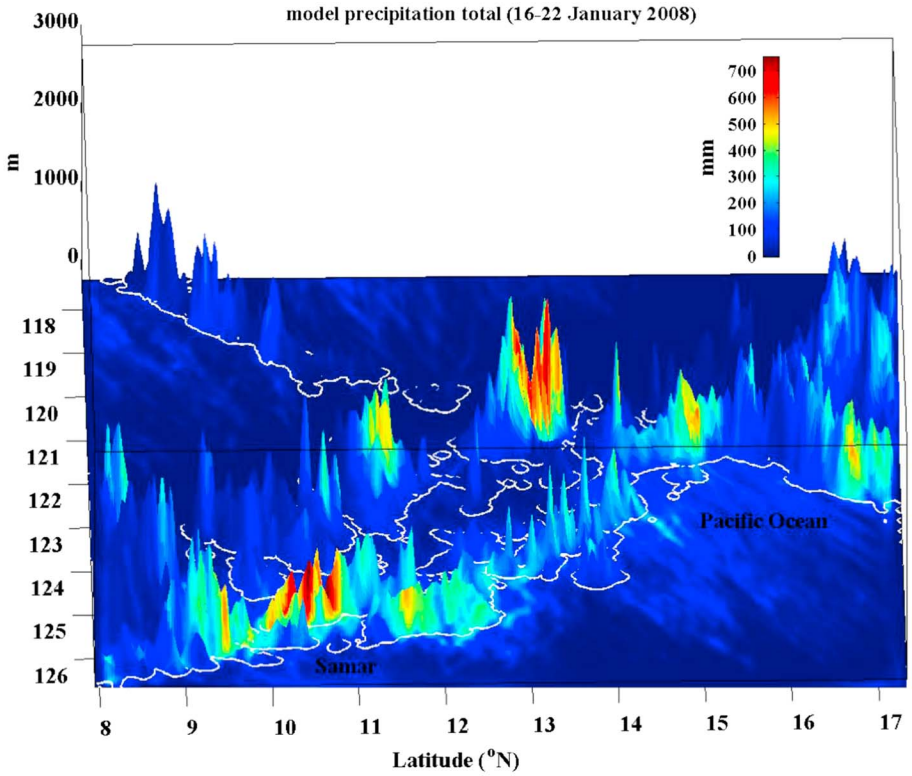

Figure 14. Model rainfall totals during MJO event 1b are contoured in color. The view is from the east toward the west. Terrain is shown in relief, and the land/ocean boundary is outlined in white.

[*Chang et al.*, 2004, 2005b]. In addition, the steep terrain of Mindoro and Panay received extreme rainfall. During event 2, which coincided with a northerly surge, there was more concentrated rainfall all along the east coast, particularly in the foothills (Figure 15). The area encompasses the island of Samar, where flooding and landslides affecting over 45,000 people was reported during event 2 [*NDCC*, 2008]. A bimodal pattern of rainfall distribution is also seen in hourly rain gauge data at 25 sites in Malaysia for 1975–2010 [*Syafrina et al.*, 2014]. Rainfall on the west (east) of Malaysia was elevated during MJOs (northeasterly monsoon).

It is interesting to note that some of the strongest rainfall occurring early in event 2 lie somewhat outside of the 40–80 day intraseasonal signal depicted in Figure 8. Orographic lifting of the intense monsoon surge and moisture convergence can create stronger precipitation. But there also exist an enhanced effect as the easterly winds blowing over the Pacific during the MJO wet phase combined with the cold surge winds [*Tangang et al.*, 2008]. Moreover, a negative to neutral IOD, as experienced in winter 2007–2008, is expected to enhance moisture advection by the MJO from the eastern Indian Ocean across the Maritime Continent [*Wilson et al.*, 2013].

The interaction of multiscale effects is explored through analyzed OLR and 850 mb height wind anomalies during the two MJO events (Figure 16). During event 1b, the MJO was in phases 6 and 7 according to the RMM index for MJO. The anomalies are similar to anomalies from Wheeler composites for this phase with positive OLR anomalies west of Sumatra and negative OLR and westerlies in the Indian Ocean. The OLR anomalies are shifted north as noted by *Lin* [2012]. It appears that the OLR anomalies are related to the Rossby-like response to the convection in the western Pacific, with the cyclonic MJO-related anomalies emanating from the equatorial Pacific farther east. Convection processes in the Pacific were amplified by the warmer SSTs during La Niña.

In event 2, the enhanced easterly component of the wind is evident (Figure 16). It represents a confluence of the northeasterly cold surge and the MJO, leading to large OLR anomalies and extreme rainfall in the vicinity of the Philippines. For event 2, the RMM index, which measures the global signal, indicates eastward

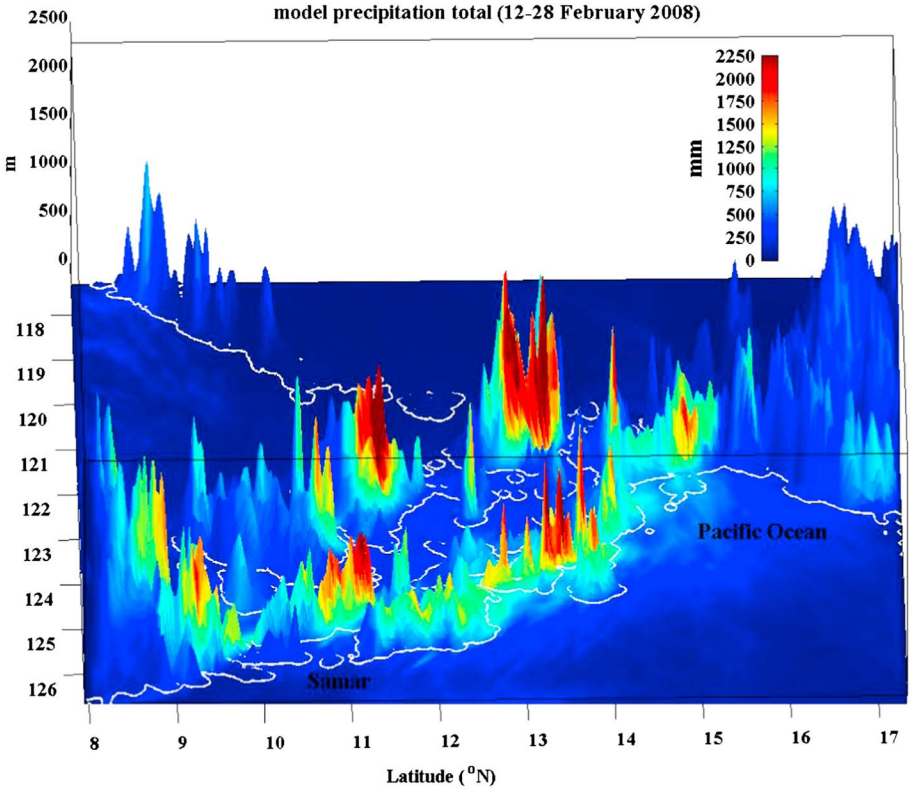

Figure 15. Same as in Figure 14 but for event 2. The scale differs from the previous plot.

propagation into the eastern Pacific in the second part of February (Figure 4), but the OLR is stationary over the Maritime Continent (Figure 8). For the RMM in February 2008, the OLR has a very small or even negative relative contribution to the index, so the local behavior of MJO convection is not consistent with the global MJO index dominated by the larger-scale wind anomaly. The strong northerly flow is indicative of the surge

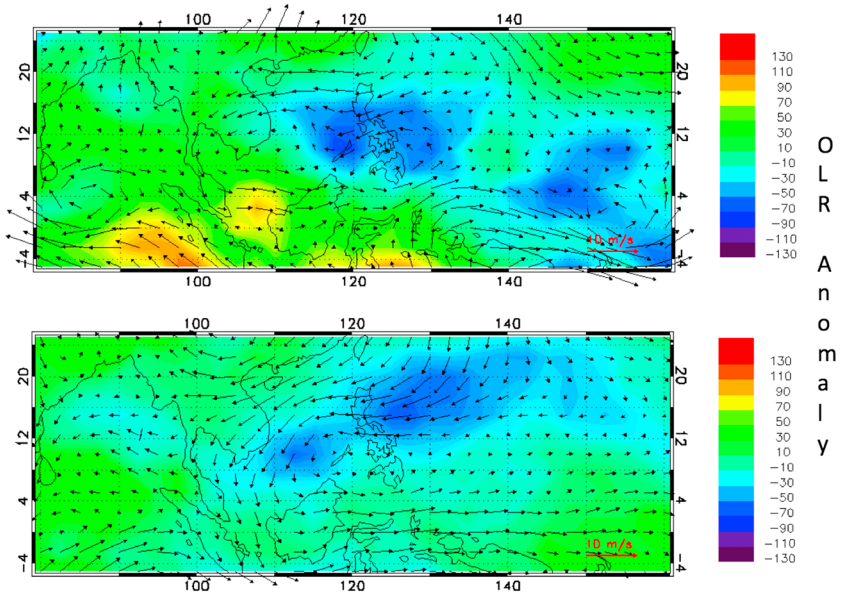

Figure 16. Analyzed OLR anomaly (in W/m^2) and 850 mb height wind anomaly for (top) event 1b and (bottom) event 2. The wind and OLR anomalies are calculated from NCEP reanalysis data. The anomalies are relative to the daily climatology, filtered with a 20–90 day filter, and averaged over the events.

and the fact that the MJO was stalled in the Maritime Continent for most of February 2008 (Figure 16). *Hong and Li* [2009] indicate that the cold surge developed in response to the enhanced convection over the Maritime Continent. In addition, they suggest that the advection of cold and dry air over the warm ocean (due to La Niña) triggered convective instability and new convection. Indeed, wet conditions extend to Sumatra during event 2 (Figure 16). *Hong and Li* [2009] further suggest that the stationary MJO behavior in February was due to the cold La Niña anomaly propagating into the western Pacific and preventing the convection from moving eastward.

5. Conclusions

The Philippines experienced extreme accumulated rainfall in winter 2007–2008. In this study, we examined the multiscale factors (interannual, seasonal, intraseasonal, and synoptic) that contributed to the elevated precipitation across the mountainous region. A confluence of factors led to the excessive rainfall. A moderate to strong La Niña is associated with uniformly rainier conditions throughout the Philippines [*Lyon et al.*, 2006]. The Indian Ocean Dipole displayed negative to neutral conditions (anomalously warmer waters in the eastern Indian Ocean) that primed the area for stronger MJO activity and enhanced moisture advection. The seasonal northeasterly monsoon enhances rainfall on the eastern side due to orographic lifting, and this mechanism was more pronounced during the second MJO event when a northerly cold surge coincided with the MJO and produced stronger moisture convergence. The MJO activity that occurred in winter 2007–2008 was the most intense since 2005, with sustained RMM amplitude in the range of 2–3.

MJO event 2 may have been instigated by a prior cold surge [*Wang et al.*, 2012] and subsequently helped initiate the prolonged northerly surge of 9–16 February 2008 by creating a heating anomaly [*Hong and Li*, 2009]. There is evidence that event 2 may have further been stalled by the La Niña conditions in the Pacific [*Hong and Li*, 2009], thus leading to enhanced prolonged precipitation in the Maritime Continent. And the northerly cold surge occurring during event 2 gained moisture via enhanced air/sea fluxes caused by warmer SSTs—the latter made warmer by a moderately strong La Niña. The linked and aggregated effects of the multiscale factors of winter 2007–2008 led to extreme rainfall and represent an important challenge for mesoscale meteorological models.

Several discrete precipitation events delivered the majority of the rainfall to the region and were identified using TRMM data. These were event 1 from 10 to 22 January 2008 and event 2 from 12 to 28 February 2008. At sites on the eastern side, rain gauge and satellite data matched the bands of rain constituting the MJO signal. The timing of modeled rain events showed approximate agreement with the observed events, and bands therein, but the magnitude of the modeled rain was overestimated for the MJO event in January (event 1b).

Not all sensing modalities captured the same signal in the same locations. For example, although TRMM revealed an MJO imprint on the overall region (Figure 8), it did not measure much rain at Calapan on the northeast coast of Mindoro in the central part of the Philippines. A rain gauge at Calapan did show rainfall there that matched the timing of MJO events 1b and 2. The model showed rainfall at Calapan in agreement with the MJO event timing, but the model overpredicted the rainfall amount for event 2.

Model fields also showed higher rainfall totals in the mountainous regions of the central islands of Mindoro and Panay. In situ ship measurements of the waters west of Mindoro in December 2007 and January 2008 confirmed much lower salinity water in the rain shadow of the island, suggesting that river runoff provided a source for the freshwater. This corresponds with the timing of the November and January (event 1) MJO episodes exhibited in Figure 8. Further evidence for this hypothesis comes from government and news reports of heavy rains, river flooding, and evacuations on Mindoro during event 2 of 12–28 February 2008.

In prior studies, COAMPS has been shown to produce reasonable correlation with observed rainfall patterns over steep terrain [*Doyle*, 1997; *Chiao and Lin*, 2003]. Based on the comparison of observed and modeled precipitation at other Philippine measurement sites like Calapan, it is likely that the rainfall totals produced by the model in the central mountainous islands, though suggested by salinity measurements and recorded in flood reports, were greater than actually occurred. Nonetheless, the ability to replicate in a 3 km resolution

two-way coupled model the approximate timing of MJO-related extreme rain events representing a confluence of multiscale and terrain factors is an important step. It suggests that just as observations of enhanced rain at the regional and local scale are beginning to be tied to MJO events [*Xavier et al.*, 2014; *Matthews et al.*, 2013], prediction at the spatial scale of the catchment basin for MJO-influenced extreme rainfall patterns is achievable.

Acknowledgments
Data contributing to the results of this research can be made available by the author upon request. COAMPS® is a registered trademark of the Naval Research Laboratory. The research support for J. Pullen was provided by Office of Naval Research (ONR) grant N00014-10-1-0300. A.L. Gordon was funded by ONR grants N00014-09-1-0582 and N00014-10-1-0426. M. Flatau and J. Doyle were supported by the Office of Naval Research (ONR) program element 0601153N. Special thanks to PAGASA for processing the station data at higher temporal frequency. Lamont-Doherty Earth Observatory contribution 7886.

References

Akasaka, I., W. Morishima, and T. Mikami (2007), Seasonal march and its spatial difference of rainfall in the Philippines, *Int. J. Climatol.*, *27*(6), 715–725.

Aldrian, E., D. Sein, D. Jacob, L. D. Gates, and R. Podzun (2005), Modelling Indonesian rainfall with a coupled regional model, *Clim. Dyn.*, *25*(1), 1–17.

Allan, R. J., et al. (2001), Is there an Indian Ocean dipole and is it independent of the El Niño–Southern Oscillation? (Doctoral dissertation, International CLIVAR Project Office).

Allard, R. A., et al. (2010), Validation test report for the Coupled Ocean/Atmosphere Mesoscale Prediction System (COAMPS) Version 5.0, *NRL/MR/7320–10-9283*, Naval Res. Lab., Oceanogr. Div., Stennis Space Cent., Miss.

Barron, C. N., A. B. Kara, P. J. Martin, R. C. Rhodes, and L. F. Smedstad (2006), Formulation, implementation and examination of vertical coordinate choices in the Global Navy Coastal Ocean Model (NCOM), *Ocean Model.*, *11*(3), 347–375.

Barros, A. P., M. Joshi, J. Putkonen, and D. W. Burbank (2000), A study of the 1999 monsoon rainfall in a mountainous region in central Nepal using TRMM products and rain gauge observations, *Geophys. Res. Lett.*, *27*(22), 3683–3686, doi:10.1029/2000GL011827.

Benedict, J., and D. A. Randall (2009), Structure of the Madden-Julian oscillation in the superparameterized CAM, *J. Atmos. Sci.*, *66*, 3277–3296.

Cabrera, O. C. (2012), Barrier layer dynamics in the Bohol and eastern Sulu Sea in response to wind and freshwater flux: Implications to phytoplankton biomass in Philippine waters, 100 pp., PhD dissertation, Univ. of the Philippines, Quezon City, Philippines.

Chang, C. P., P. A. Harr, J. McBride, and H. H. Hsu (2004), Maritime Continent monsoon: Annual cycle and boreal winter variability, *East Asian Monsoon*, *2*, 107.

Chang, C. P., P. A. Harr, and H. J. Chen (2005a), Synoptic disturbances over the equatorial South China Sea and western Maritime Continent during boreal winter, *Mon. Weather Rev.*, *133*(3), 489–503.

Chang, C. P., Z. Wang, J. McBride, and C. H. Liu (2005b), Annual cycle of Southeast Asia: Maritime Continent rainfall and the asymmetric monsoon transition, *J. Clim.*, *18*(2), 281–301.

Chang, C. P., Z. Wang, and H. Hendon (2006), The Asian winter monsoon, in *The Asian Monsoon*, edited by B. Wang, pp. 89–127, Springer, Berlin.

Chen, B., and M. Yanai (2000), Comparison of the Madden-Julian oscillation (MJO) during the TOGA COARE IOP with a 15 year climatology, *J. Geophys. Res.*, *105*(D2), 2139–2149, doi:10.1029/1999JD901045.

Chen, C.-S., Y.-L. Lin, H.-T. Zeng, C.-Y. Chen, and C.-L. Liu (2013), Orographic effects on heavy rainfall events over northeastern Taiwan during the northeasterly monsoon season, *Atmos. Res.*, *122*, 310–335.

Chen, S., et al. (2015), A Study of CINDY/DYNAMO MJO suppressed phase, *J. Atmos. Sci.*, doi:10.1175/JAS-D-13-0348.1.

Chiao, S., and Y. L. Lin (2003), Numerical modeling of an orographically enhanced precipitation event associated with Tropical Storm Rachel over Taiwan, *Weather Forecasting*, *18*(2), 325–344.

Couto, F. T., R. Salgado, and M. J. Costa (2012), Analysis of intense rainfall events on Madeira Island during the 2009/2010 winter, *Nat. Hazards Earth Syst. Sci.*, *12*(7), 2225–2240.

Doyle, J. D. (1997), The influence of mesoscale orography on a coastal jet and rainband, *Mon. Weather Rev.*, *125*(7), 1465–1488.

Flatau, M., P. J. Flatau, P. Phoebus, and P. P. Niiler (1997), The feedback between equatorial convection and local radiative and evaporative processes: The implications for intraseasonal oscillations, *J. Atmos. Sci.*, *54*, 2373–2386.

Fu, X., B. Yang, Q. Bao, and B. Wang (2008), Sea surface temperature feedback extends the predictability of tropical intraseasonal oscillation, *Mon. Weather Rev.*, *136*(2), 577.

Fu, X., J.-Y. Lee, P.-C. Hsu, H. Taniguchi, B. Wang, W. Wang, and S. Weaver (2013), Multimodel MJO forecasting during DYNAMO/CINDY period, *Clim. Dyn.*, *41*, 1067–1081.

Gordon, A. L., and C. L. Villanoy (2011), The oceanography of the Philippine Archipelago: Introduction to the special issue, *Oceanography*, *24*(1), 13.

Gordon, A. L., J. Sprintall, and A. Ffield (2011), Regional oceanography of the Philippine Archipelago, *Oceanography*, *24*, 14–27, doi:10.5670/oceanog.2011.01.

Gottschalck, J., et al. (2010), A framework for assessing operational Madden-Julian oscillation forecasts: A CLIVAR MJO working group project, *Bull. Am. Meteorol. Soc.*, *91*(9), 1247–1258.

Grabowski, W. W. (2006), Impact of explicit atmosphere-ocean coupling on MJO-like coherent structures in idealized aquaplanet simulations, *J. Atmos. Sci.*, *63*(9), 2289.

Hattori, M., S. Mori, and J. Matsumoto (2011), The cross-equatorial northerly surge over the Maritime Continent and its relationship to precipitation patterns (Special issue on MAHASRI: Monsoon Asian hydro-atmosphere scientific research and prediction initiative), *J. Meteorol. Soc. Jpn.*, *89*, 27–47.

Hodur, R. M. (1997), The Naval Research Laboratory's Coupled Ocean/Atmosphere Mesoscale Prediction System (COAMPS), *Mon. Weather Rev.*, *125*(7), 1414–1430.

Hong, C.-C., and T. Li (2009), The extreme cold anomaly over Southeast Asia in February 2008: Roles of ISO and ENSO, *J. Clim.*, *22*, doi:10.1175/2009JCLI2864.1.

Huffman, G. J., R. F. Adler, D. T. Bolvin, G. Gu, E. J. Nelkin, K. P. Bowman, Y. Hong, E. F. Stocker, and D. B. Wolff (2007), The TRMM multisatellite precipitation analysis (TMPA): Quasi-global, multiyear, combined-sensor precipitation estimates at fine scales, *J. Hydrometeorol.*, *8*, 38–55.

Hung, M. P., J.-L. Lin, W. Wang, D. Kim, T. Shinoda, and S. J. Weaver (2013), MJO and convectively coupled equatorial waves simulated by CMIP5 climate models, *J. Clim.*, *26*, 6185–6214.

Ichikawa, H., and T. Yasunari (2007), Propagating diurnal disturbances embedded in the Madden-Julian oscillation, *Geophys. Res. Lett.*, *34*, L18811, doi:10.1029/2007GL030480.

Iguchi, T., T. Kozu, R. Meneghini, J. Awaka, and K. I. Okamoto (2000), Rain-profiling algorithm for the TRMM precipitation radar, *J. Appl. Meteorol.*, *39*(12), 2038–2052.

Jamandre, C. A., and G. T. Narisma (2013), Spatio-temporal validation of satellite-based rainfall estimates in the Philippines, *Atmos. Res.*, *122*, 599–608.
Juneng, L., F. T. Tangang, and C. J. C. Reason (2007), Numerical case study of an extreme rainfall event during 9–11 December 2004 over the east coast of Peninsular Malaysia, *Meteorol. Atmos. Phys.*, *98*(1–2), 81–98.
Kanamori, H., T. Yasunari, and K. Kuraji (2013), Modulation of the diurnal cycle of rainfall associated with the MJO observed by a dense hourly rain gauge network at Sarawak, Borneo, *J. Clim.*, *26*(13), 4858–4875.
Kim, H., C. D. Hoyos, P. J. Webster, and I. Kang (2008), Sensitivity of MJO simulation and predictability to sea surface temperature variability, *J. Clim.*, *21*(20), 5304.
Lin, L. (2012), The ISO events in the winter of 2007, *Atmos. Ocean. Sci. Lett.*, *5*(2), 151–155.
Lyon, B., and S. J. Camargo (2009), The seasonally-varying influence of ENSO on rainfall and tropical cyclone activity in the Philippines, *Clim. Dyn.*, *32*(1), 125–141.
Lyon, B., H. Cristi, E. R. Verceles, F. D. Hilario, and R. Abastillas (2006), Seasonal reversal of the ENSO rainfall signal in the Philippines, *Geophys. Res. Lett.*, *33*, L24710, doi:10.1029/2006GL028182.
Madden, R., and P. R. Julian (1971), Detection of a 40–50 day oscillation in the zonal wind in the Tropical Pacific, *J. Atmos. Sci.*, *28*, 702–708.
Majda, A. J., and S. N. Stechmann (2009), The skeleton of tropical intraseasonal oscillations, *Proc. Natl. Acad. Sci. U.S.A.*, *106*(21), 8417–8422.
Matthews, A. J., G. Pickup, S. C. Peatman, P. Clews, and J. Martin (2013), The effect of the Madden-Julian oscillation on station rainfall and river level in the Fly River system, Papua New Guinea, *J. Geophys. Res. Atmos.*, *118*, 10–926.
May, P. W., J. D. Doyle, J. Pullen, and L. David (2011), Two-way coupled atmosphere-ocean modeling of the PhilEx intensive observational period, *Oceanography*, *24*(1), 48–57.
Miura, H., M. Satoh, T. Nasuno, A. T. Noda, and K. Oouchi (2007), A Madden-Julian oscillation event realistically simulated by a global cloud-resolving model, *Science*, *318*(5857), 1763–1765.
Nakazawa, T. (1988), Tropical super clusters within intraseasonal variations over the western Pacific, *J. Meteorol. Soc. Jpn.*, *66*(6), 823–839.
National Disaster Coordination Council (2008), Update Report re: Flooding and Landslide in Region VIII & IVB as of 12:00 Noon 19 February 2008.
Peatman, S. C., A. J. Matthews, and D. P. Stevens (2013), Propagation of the Madden-Julian oscillation through the Maritime Continent and scale interaction with the diurnal cycle of precipitation, *Q. J. R. Meteorol. Soc.*, doi:10.1002/qj.2161.
Pegion, K., and B. P. Kirtman (2008a), The impact of air-sea interactions on the predictability of the tropical intraseasonal oscillation, *J. Clim.*, *21*(22), 5870.
Pegion, K., and B. P. Kirtman (2008b), The impact of air-sea interactions on the simulation of tropical intraseasonal variability, *J. Clim.*, *21*(24), 6616.
Pullen, J., J. D. Doyle, P. W. May, C. Chavanne, P. Flament, and R. Arnone (2008), Monsoon surges trigger oceanic eddy formation and propagation in the lee of the Philippine Islands, *Geophys. Res. Lett.*, *35*, L07604, doi:10.1029/2007GL033109.
Pullen, J., A. L. Gordon, J. Sprintall, C. M. Lee, M. A. Alford, J. D. Doyle, and P. W. May (2011), Atmospheric and oceanic processes in the vicinity of an island strait, *Oceanography*, *24*(1), 112–121.
Ramage, C. S. (1968), Role of a tropical "maritime continent" in the atmospheric circulation, *Mon. Weather Rev.*, *96*(6), 365–370.
Shinoda, T., T. G. Jensen, M. Flatau, and S. Chen (2013), Surface wind and upper-ocean variability associated with the Madden-Julian oscillation simulated by the Coupled Ocean-Atmosphere Mesoscale Prediction System (COAMPS), *Mon. Weather Rev.*, *141*(7), 2290–2307.
Syafrina, A. H., M. D. Zalina, and L. Juneng (2014), Historical trend of hourly extreme rainfall in peninsular Malaysia, *Theor. Appl. Climatol.*, *120*, 259–285.
Tangang, F. T., L. Juneng, E. Salimun, P. N. Vinayachandran, Y. K. Seng, C. J. Reason, S. K. Behera, and T. Yasunari (2008), On the roles of the northeast cold surge, the Borneo vortex, the Madden-Julian oscillation, and the Indian Ocean Dipole during the extreme 2006/2007 flood in southern Peninsular Malaysia, *Geophys. Res. Lett.*, *35*, L14S07, doi:10.1029/2008GL033429.
Villafuerte, M. Q., II, J. Matsumoto, I. Akasaka, H. G. Takahashi, H. Kubota, and T. A. Cinco (2014), Long-term trends and variability of rainfall extremes in the Philippines, *Atmos. Res.*, *137*, 1–13.
Wang, L., K. Koderab, and W. Chen (2012), Observed triggering of tropical convection by a cold surge: Implications for MJO initiation, *Q. J. R. Meteorol. Soc.*, *138*, 1740–1750.
Wheeler, M. C. (2008), Seasonal climate summary southern hemisphere (summer 2007-08): Mature La Niña, an active MJO, strongly positive SAM, and highly anomalous sea-ice, *Aust. Meteorol. Mag.*, *57*(4), 379.
Wheeler, M. C., and H. H. Hendon (2004), An all-season real-time multivariate MJO index: Development of an index for monitoring and prediction, *Mon. Weather Rev.*, *132*(8), 1917–1932.
Wilson, E. A., A. L. Gordon, and D. Kim (2013), Observations of the Madden-Julian oscillation during Indian Ocean dipole events, *J. Geophys. Res. Atmos.*, *118*, 2588–2599.
Woolnough, S. J., F. Vitart, and M. A. Balmaseda (2007), The role of the ocean in the Madden-Julian oscillation: Implications for MJO prediction, *Q. J. R. Meteorol. Soc.*, *133*(622), 117.
Wu, C. H., and H. H. Hsu (2009), Topographic influence on the MJO in the Maritime Continent, *J. Clim.*, *22*(20), 5433–5448.
Wu, P., A. A. Arbain, S. Mori, J. I. Hamada, M. Hattori, F. Syamsudin, and M. D. Yamanaka (2013), The effects of an active phase of the Madden-Julian oscillation on the extreme precipitation event over western Java Island in January 2013, *SOLA*, *9*, 79–83.
Xavier, P., R. Rahmat, W. K. Cheong, and E. Wallace (2014), Influence of Madden-Julian oscillation on Southeast Asia rainfall extremes: Observations and predictability, *Geophys. Res. Lett.*, *41*, 4406–4412, doi:10.1002/2014GL060241.
Yoneyama, K., C. Zhang, and C. N. Long (2013), Tracking pulses of the Madden-Julian oscillation, *Bull. Am. Meteorol. Soc.*, *94*(12), 1871–1891.
Zhang, C. (2005), The Madden-Julian oscillation, *Rev. Geophys*, *43*, RG2003, doi:10.1029/2004RG000158.
Zhang, C., M. Dong, S. Gualdi, H. H. Hendon, E. D. Maloney, A. Marshall, K. R. Sperber, and W. Wang (2006), Simulations of the Madden-Julian oscillation in four pairs of coupled and uncoupled global models, *Clim. Dyn.*, *27*(6), 573.